

AD-A082 235

ARMY ENGINEER TOPOGRAPHIC LABS FORT BELVOIR VA
DETECTION OF SIGNAL SIGNATURES OF CARTOGRAPHIC FEATURES, (U)
JAN 80 P CHEN, W SEEMULLER
ETL-R006

F/G 8/2

UNCLASSIFIED

NL

1 OF 1
AD
ADDRESS

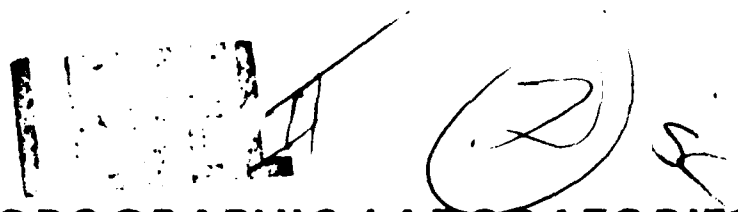


END
DATE
FILMED
4-80
DTIC

U.S. ARMY

ENGINEER TOPOGRAPHIC LABORATORIES

FORT BELVOIR, VIRGINIA



ADA 082235

ETL-R-006

DETECTION OF SIGNAL SIGNATURES OF CARTOGRAPHIC FEATURES

by

Pi-Fuay Chen and William Seemuller

Approved for public release; distribution unlimited



80 20 062

| REPORT DOCUMENTATION PAGE | | READ INSTRUCTIONS BEFORE COMPLETING FORM |
|--|-----------------------|--|
| 1. REPORT NUMBER R-006 | 2. GOVT ACCESSION NO. | 3. RECIPIENT'S CATALOG NUMBER |
| 4. TITLE (and Subtitle) DETECTION OF SIGNAL SIGNATURES OF CARTOGRAPHIC FEATURES | | 5. TYPE OF REPORT & PERIOD COVERED Paper |
| | | 6. PERFORMING ORG. REPORT NUMBER |
| 7. AUTHOR(s) Dr. Pi-Fuay/Chen and Mr. William/Seemuller | | 8. CONTRACT OR GRANT NUMBER(s) |
| 9. PERFORMING ORGANIZATION NAME AND ADDRESS USA Engineer Topographic Laboratories Fort Belvoir, VA 22060 | | 10. PROGRAM ELEMENT, PROJECT, TASK AREA & WORK-UNIT NUMBERS 15111 |
| 11. CONTROLLING OFFICE NAME AND ADDRESS see 9 above | | 12. REPORT DATE 11 17 Jan 80 |
| 14. MONITORING AGENCY NAME & ADDRESS (if different from Controlling Office) JL ETL-770 | | 13. NUMBER OF PAGES |
| | | 15. SECURITY CLASS. (of this report) |
| | | 15a. DECLASSIFICATION/DOWNGRADING SCHEDULE |
| 16. DISTRIBUTION STATEMENT (of this Report) Approved for public release; distribution unlimited | | |
| 17. DISTRIBUTION STATEMENT (of the abstract entered in Block 20, if different from Report) | | |
| 18. SUPPLEMENTARY NOTES | | |
| 19. KEY WORDS (Continue on reverse side if necessary and identify by block number) | | |
| 1. Wash Transform 2. Sensing Array 3. Signal Signature 4. Cartographic Features Extraction 5. Pattern Recognition | | |
| 20. ABSTRACT (Continue on reverse side if necessary and identify by block number) A semi-automated technique was developed for extracting and recognizing cartographic features, such as, road intersections, straight line roads, and rectangular objects from aerial photographs. The method uses the Wash transform processing technique, and was implemented with an electronic experimental system consisting of a solid-state sensor array, a minicomputer, and a computer-controlled translational stage as the imagery holder. Successful experimental results were obtained for a selected set of cartographic features of the types described above. This feature extractor will be integrated in parallel with other feature extractors, | | |

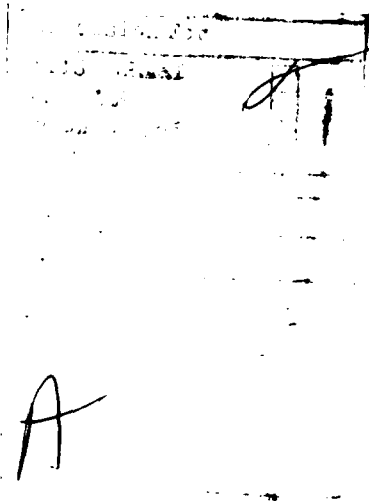
4103192

UNCLASSIFIED

SECURITY CLASSIFICATION OF THIS PAGE(When Data Entered)

→ WHICH ARE TO BE DEVELOPED IN THE FUTURE, TO BECOME A TOTAL AUTOMATED FEATURE EXTRACTION SYSTEM.

A METHOD FOR DETECTING THE DECOMPOSED SIGNAL SIGNATURES REPRESENTING CARTOGRAPHIC FEATURES USING ANALOG PROCESSORS IS DESCRIBED. FINALLY, CONCLUSIONS ARE ARE GIVEN. ↖



UNCLASSIFIED

SECURITY CLASSIFICATION OF THIS PAGE(When Data Entered)

*CHEN and SEEMULLER

TITLE: Detection of Signal Signatures of Cartographic Features

Pi-Fuay Chen and William W. Seemuller
U. S. Army Engineer Topographic Laboratories
Fort Belvoir, Virginia 22060

ABSTRACT:

A semi-automated technique was developed for extracting and recognizing cartographic features, such as, road intersections, straight line roads, and rectangular objects from aerial photographs. The method uses the Walsh transform processing technique, and was implemented with an electronic experimental system consisting of a solid-state sensor array, a minicomputer, and a computer-controlled translational stage as the imagery holder. Successful experimental results were obtained for a selected set of cartographic features of the types described above. This feature extractor will be integrated in parallel with other feature extractors, which are to be developed in the future, to become a total automated feature extraction system.

A method for detecting the decomposed signal signatures representing cartographic features using analog processors is described. Finally, conclusions are given.

BIOGRAPHY:

PRESENT ASSIGNMENT: Electronics Engineer, U. S. Army Engineer Topographic Laboratories

PAST EXPERIENCE: Assistant Engineer, Taipei Telecommunication Office, Taipei, Taiwan, 1956-1960; Engineer and Senior Engineer, International Telephone and Telegraph Corporation, Raleigh, N. C. 1963-1966; Graduate Research Assistant, Research Laboratories for Engineering and Applied Sciences, University of Virginia, 1966-1968; Assistant Professor, George Washington University, Washington, D. C. 1968-1969.

DEGREES HELD: Equivalent BSEE, Taipei Institute of Technology Taipei, Taiwan, 1956; MSEE, Virginia Polytechnic Institute, Blacksburg, Virginia, 1963; DSc., University of Virginia, Charlottesville, Virginia, 1968.

*CHEN and SEEMULLER

DETECTION OF SIGNAL SIGNATURES
OF CARTOGRAPHIC FEATURES

*PI-FUAY CHEN, DSC
WILLIAM W. SEEMULLER, PHD
U.S. ARMY ENGINEER TOPOGRAPHIC LABORATORIES
FORT BELVOIR, VA 22060

Currently photo interpretation and terrain image identification for military applications is performed manually. This work is time consuming and costly. The work described below is a first step to aiding or semi-automating some of these labor intensive tasks.

A semi-automated technique for extracting a selected set of cartographic features such as, road intersections, straight line roads, and rectangular objects from aerial photographs was recently developed at the U.S. Army Engineer Topographic Laboratories (USAETL) using the Walsh transform. The discrete function (Walsh) transform was chosen because of its simplicity (Walsh functions are only two-valued) resulting in simple implementation, and because Walsh functions conform to the selected set of the cartographic features. Since the Walsh transform coefficients were produced by using Walsh functions having alternate magnitudes (either +1 or -1) at different sequences, the Walsh transform coefficients are also decomposed spectral components of the signal signature of the input aerial photographic images.

The technique was investigated in two ways as follows:
(1) Using a 32-by 32-element solid state sensor array to convert aerial imagery into an electronic signal which was processed in a minicomputer to yield Walsh transforms of the image [1]. (2) A prototype image spectrum analyzer (PISA) was developed which utilizes a large size plasma discharge device (8.5-by 8.5-inch illuminating area with 512 electrodes each in both x and y directions) to generate two-dimensional Walsh function patterns, and produce 512 by 512 Walsh coefficients in 14 seconds [2]. The PISA produced successful results

*CHEN and SEEMULLER

for a selected set of targets representing man-made cartographic features of the type stated above. The sensor array-minicomputer system provides a variable image threshold which results in better control of the input images. The cartographic features as described with background scenes and noise were extracted successfully from aerial imagery.

The sensor array-minicomputer system described in [1] was further expanded to incorporate a classification scheme to become a semi-automated cartographic feature extraction and recognition system. This paper describes this experimental system which was implemented with a solid state sensor array as an opto-electronic converter, a minicomputer as a signal processor to perform the functions of feature extraction and recognition, and a computer-controlled translational stage as the imagery holder. Successful extraction and recognition results for the selected set of cartographic features using this experimental system are presented. An alternate method for detecting the decomposed signal signatures representing cartographic features using analog signal processors is briefly described, and conclusions are given.

SYSTEM CONFIGURATION

A system that will produce signal signatures from the grey-shade distribution of a photo transparency in a short time and with recognizable resolution was developed. The block diagram of such a system is shown in Figure 1.

A 9- by 9-inch aerial transparency is illuminated by a white light source, and a section of the image is projected on a Reticon 32- by 32-element solid state array with a lens. The array converts the optical energy of the image into a video signal. The array timing and video signals, after being conditioned and digitized by the computer interface are sliced by the Hewlett-Packard (HP) 2100 minicomputer into two values, "on" and "off." The threshold value of the slicing is variable, which provides a very convenient means for isolating signals representing the selected feature image from the unwanted background noise. The "on" value of the video is arbitrarily set to "100" and "off" to "0," and the quantized image is printed by a line printer as a two-dimensional binary array of 32 by 32 pixels that represent the spatial signal signature of the selected topographic features. The sliced signal is transformed into a 32 by 32 Walsh matrix with a conventional Walsh transform algorithm in the computer. This algorithm implements the two-dimensional discrete Walsh transform [3],

*CHEN and SEEMULLER

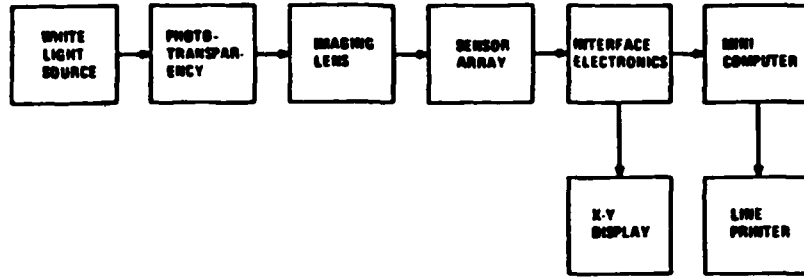


Figure 1. System Block Diagram

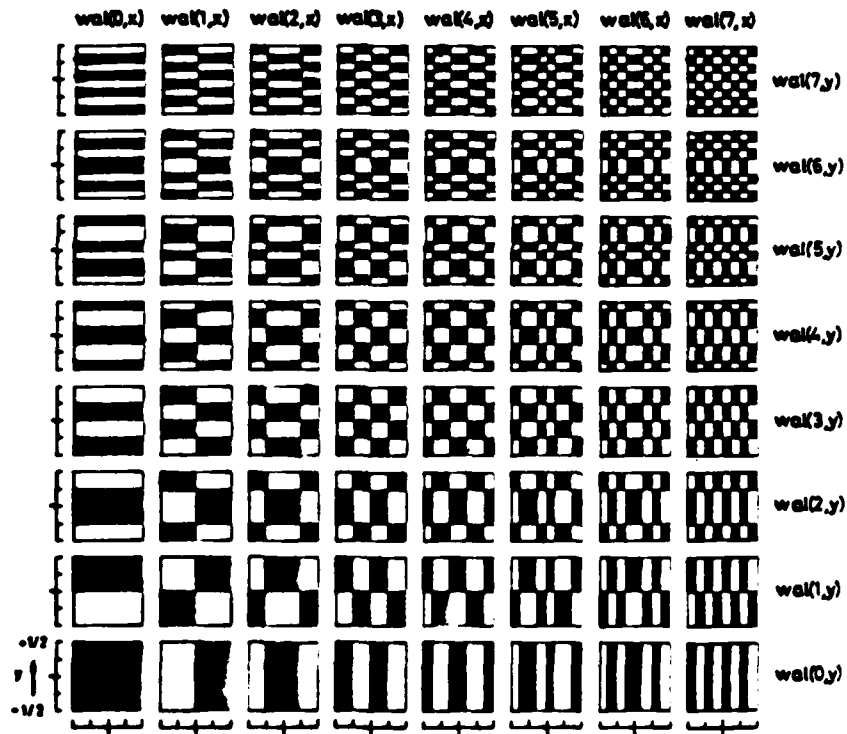


Figure 2. First 8-by 8-Order, Two-Dimensional Walsh Functions

*CHEN and SEEMULLER

$$A(i,j) = \frac{1}{1024} \sum_{x=1}^{32} \sum_{y=1}^{32} f(x,y) \text{Wal}(i,x) \text{Wal}(j,y)$$

where $f(x,y)$ is the image binary array, $\text{Wal}(i,x)$ $\text{Wal}(j,y)$ is the two-dimensional Walsh function of order i and j , and x,y,i , and j take values from 1 through 32. By sequentially changing the order of the Walsh function, the complete set (32 by 32) of the Walsh transform coefficients was obtained. The Walsh functions used are permanently stored in the minicomputer. Figure 2 shows the first 8 by 8 order, two-dimensional Walsh functions in the x and y ranges of $-\frac{1}{2}$ to $+\frac{1}{2}$. The black areas indicate +1 in magnitude, and white -1.

Since the Walsh transform coefficients are produced by using Walsh functions having spatially alternating magnitudes (from +1 to -1) at different sequences, the Walsh transform coefficients represent the decomposed spectral components of the signal signature of the input signal. These spectral components were divided by a convenient constant, in this case 1,024, which is the number of pixels in a frame for normalization purposes. The entire normalized set of the spectral components was printed out by the line printer.

A detection scheme was implemented based on the uniqueness of the Walsh transform of each feature under consideration. At first a reference signal signature was established for each cartographic feature of the entire selected set. The test imagery after being transformed into the Walsh domain was then compared to each reference signal signature sequentially, and classification was made. Since cartographic features may appear in a variety of locations in the window of inspection (for this case, the active surface of the solid state array), and because Walsh transforms are neither translationally nor rotationally invariant, two or more reference signal signatures are required for each class of cartographic feature to avoid misclassification. With this modification, four classes out of the entire seven cartographic feature classes selected were recognized without error regardless of their location with respect to the window. The rest of the features were also classified correctly in the majority of locations. However, misclassification occurred when these feature classes were located very close to the corners of the window. Both the magnitude of a single Walsh transform coefficient (or the sum of a row or column of the transform coefficients), and the ratio of each significant coefficient to $A(1,1)$ or $A(2,1)$ or $A(3,1)$ were used as reference signal signatures for classification. At the end of each classification, the translational stage was automatically moved a predetermined number of steps in the x and y directions, and the new

*CHEN and SEEMULLER

segment of the test image was projected on the surface of the array. The same procedure described above was repeated.

EXPERIMENTAL RESULTS

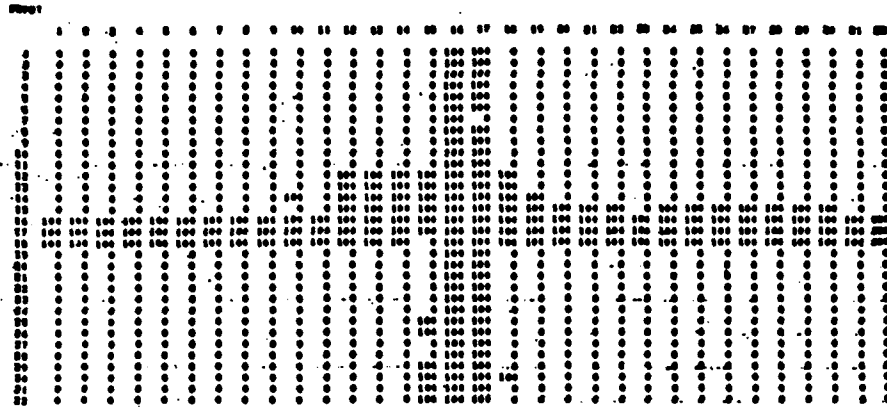
A selected set of images containing man-made cartographic features such as, road intersections, straight line roads, and rectangular objects from an aerial photo transparency and a few mask patterns were used as input test patterns for the system. The spatial signal signatures, the associated Walsh transforms (decomposed spectral signal signatures) and the classification results are shown for each of the test images. Figures 3 through 6 indicate the results for a road intersection, a horizontal line road, a vertical line road, and a rectangular object. These cartographic features were placed at various positions with respect to the window of inspection. They were detected and classified correctly regardless of their location with respect to the window. The results for these different positions are not shown because of the limited paper size. Figure 7 shows the detection results for a diagonally oriented road intersection. It is found that the correct classification was obtained for a majority of feature locations with respect to the window. However, it was misclassified as a diagonally oriented line road only when the center of the diagonally oriented road intersection was positioned against four corners of the window (not shown). This is because the energy contributed by one branch of the diagonally oriented road intersection is much stronger than that of the other branch. Figures 8 and 9 are the results of the classification for the diagonally oriented line roads having 45- and 135-degree angles with respect to the x-axis of the window. They are recognized correctly in a majority of locations. It was noted that these roads were not recognized when they moved towards the corners of the window (not shown). A few other aerial photo-transparencies containing relatively complicated scenes were also tried. Most of them were recognized correctly, while some were misclassified, or were not recognized. The results are not shown, in the interest of brevity. The overall results indicate that the Walsh transform processing technique is quite successful for detecting well-defined linear man-made cartographic features. Nearly 90 percent recognition accuracy was obtained for a set of selected cartographic features of the classes described. A rotational dimension may be incorporated in the future to refine the method for detecting the above cartographic features at various angles with respect to the axes of the window.

This system or feature extractor will be integrated in parallel with other feature extractors which are to be developed in the future

*CHEN and SEEMULLER

THIS PAGE IS BEST QUALITY FROM ORIGINAL
FROM COPY FURNISHED TO DDC

MAY 16 1979 8:44



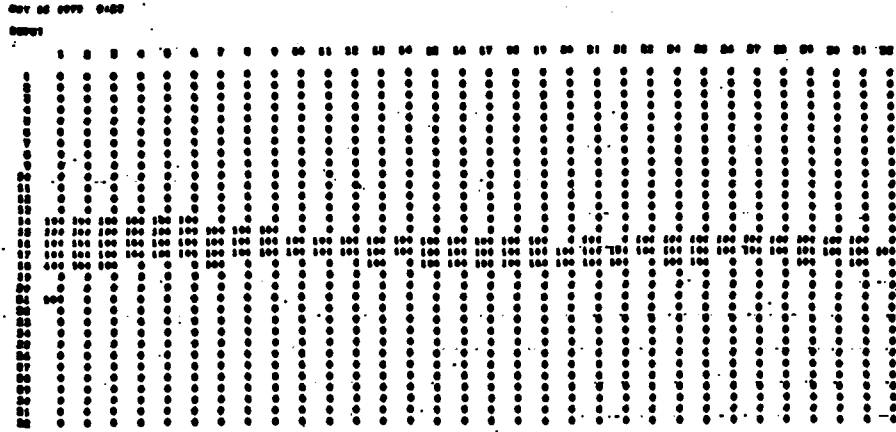
MAY 16 1979 8:44

TRANSFORM

| | 1 | 2 | 3 | 4 | 5 | 6 | 7 | 8 | 9 | 10 | 11 | 12 | 13 | 14 | 15 | 16 |
|----|-----|----|----|----|----|---|----|---|----|----|----|----|----|----|----|----|
| 1 | 18 | 0 | -8 | -1 | 7 | 0 | -7 | 0 | 5 | 0 | -5 | 0 | 6 | 0 | -6 | 0 |
| 2 | 0 | 0 | -1 | 0 | 0 | 0 | 0 | 0 | -1 | 0 | 0 | 1 | 0 | 0 | 0 | 0 |
| 3 | -11 | 0 | 0 | 0 | 0 | 0 | 0 | 0 | 2 | 1 | -1 | -1 | 1 | 0 | 0 | -1 |
| 4 | -1 | 0 | 3 | 1 | -1 | 0 | 2 | 0 | 0 | 0 | 0 | 0 | 0 | 0 | 0 | 0 |
| 5 | 11 | 0 | 0 | 0 | 0 | 0 | 0 | 0 | 0 | 0 | 0 | 0 | 0 | 0 | 1 | 0 |
| 6 | 0 | 0 | -1 | 0 | 0 | 0 | 0 | 0 | 0 | 0 | 0 | 0 | 0 | 0 | 0 | 0 |
| 7 | -10 | 0 | 0 | 0 | 0 | 0 | 0 | 0 | 1 | 0 | -1 | 0 | 1 | 0 | 0 | 0 |
| 8 | 0 | 0 | 1 | 0 | 0 | 0 | 1 | 0 | 0 | 0 | 0 | 0 | 0 | 0 | 0 | 0 |
| 9 | 8 | -1 | 1 | 0 | -1 | 0 | 1 | 0 | 0 | 1 | 0 | 0 | 0 | 0 | 0 | 0 |
| 10 | -3 | -1 | 1 | 0 | 0 | 0 | 0 | 0 | 0 | 0 | 0 | 0 | 0 | 0 | 0 | 0 |
| 11 | -8 | 2 | -1 | 0 | 1 | 0 | -1 | 0 | 0 | 0 | 0 | 0 | 0 | 0 | 0 | 0 |
| 12 | 2 | 1 | 0 | 0 | 0 | 0 | 0 | 0 | 0 | -1 | 0 | 0 | 0 | 0 | 0 | 0 |
| 13 | 9 | -1 | 1 | 0 | -1 | 0 | 0 | 0 | -1 | 0 | 0 | 0 | 0 | 0 | 0 | 0 |
| 14 | -1 | 0 | 0 | 0 | 0 | 0 | 0 | 0 | 0 | 0 | 0 | 0 | 0 | 0 | 0 | 0 |
| 15 | -9 | 0 | 0 | 0 | 0 | 0 | 0 | 0 | 0 | 0 | 0 | 0 | 0 | 0 | 0 | 0 |
| 16 | 2 | 0 | 0 | 0 | 0 | 0 | 0 | 0 | 0 | 0 | 0 | 0 | 0 | 0 | 0 | 0 |

ROAD INTERSECTION

Figure 3. Spatial Signal Signature, Walsh Transform, and Classification Result for Road Intersection.



MAY 15 1979 9:23

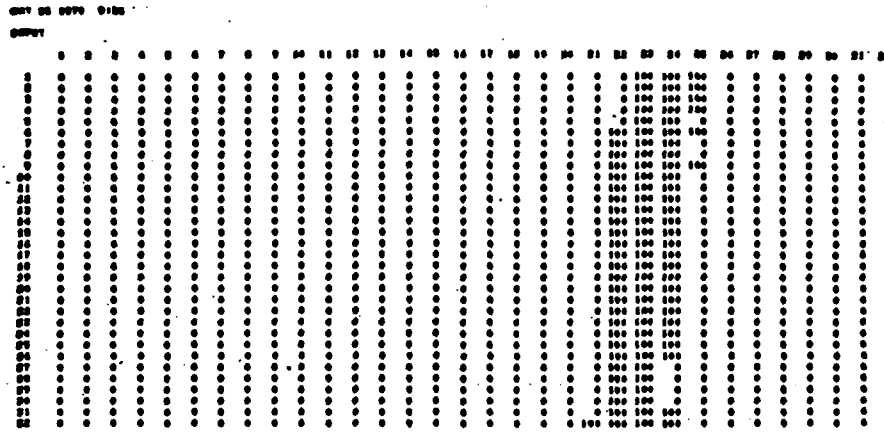
TRANSFORM

| | 1 | 2 | 3 | 4 | 5 | 6 | 7 | 8 | 9 | 10 | 11 | 12 | 13 | 14 | 15 | 16 |
|----|----|----|----|----|----|---|---|---|---|----|----|----|----|----|----|----|
| 1 | 9 | 1 | 1 | 1 | 0 | 0 | 0 | 0 | 0 | 0 | 0 | 0 | 0 | 0 | 0 | 0 |
| 2 | 0 | 1 | 1 | 0 | 0 | 0 | 0 | 0 | 0 | 0 | 0 | 0 | 0 | 0 | 0 | 0 |
| 3 | -9 | -1 | -1 | -1 | 0 | 0 | 0 | 0 | 0 | 0 | 0 | 0 | 0 | 0 | 0 | 0 |
| 4 | 0 | -1 | -1 | 0 | 0 | 0 | 0 | 0 | 0 | 0 | 0 | 0 | 0 | 0 | 0 | 0 |
| 5 | 8 | 1 | 0 | 1 | 0 | 0 | 0 | 0 | 0 | 0 | 0 | 0 | 0 | 0 | 0 | 0 |
| 6 | 0 | 2 | 1 | 0 | 0 | 0 | 0 | 0 | 0 | 0 | 0 | 0 | 0 | 0 | 0 | 0 |
| 7 | -8 | -1 | 0 | -1 | 0 | 0 | 0 | 0 | 0 | 0 | 0 | 0 | 0 | 0 | 0 | 0 |
| 8 | 0 | -2 | -1 | 0 | 0 | 0 | 0 | 0 | 0 | 0 | 0 | 0 | 0 | 0 | 0 | 0 |
| 9 | 7 | 0 | 0 | 0 | 0 | 0 | 0 | 0 | 0 | 0 | 0 | 0 | 0 | 0 | 0 | 0 |
| 10 | -1 | 0 | 0 | 0 | 0 | 0 | 0 | 0 | 0 | 0 | 0 | 0 | 0 | 0 | 0 | 0 |
| 11 | -7 | 0 | 0 | 0 | 0 | 0 | 0 | 0 | 0 | 0 | 0 | 0 | 0 | 0 | 0 | 0 |
| 12 | 1 | 0 | 0 | 0 | 0 | 0 | 0 | 0 | 0 | 0 | 0 | 0 | 0 | 0 | 0 | 0 |
| 13 | 8 | 0 | 0 | 0 | 0 | 0 | 0 | 0 | 0 | 0 | 0 | 0 | 0 | 0 | 0 | 0 |
| 14 | -1 | 0 | 0 | 0 | -1 | 0 | 0 | 0 | 0 | 0 | 0 | 0 | 0 | 0 | 0 | 0 |
| 15 | -8 | 0 | 0 | 0 | 0 | 0 | 0 | 0 | 0 | 0 | 0 | 0 | 0 | 0 | 0 | 0 |
| 16 | 1 | 0 | 0 | 0 | 1 | 0 | 0 | 0 | 0 | 0 | 0 | 0 | 0 | 0 | 0 | 0 |

HORIZONTAL LINE ROAD

Figure 4. Spatial Signal Signature, Walsh Transform, and Classification Result for Horizontal Line Road.

THIS PAGE IS UNCLASSIFIED PRACTICABLE
FROM COPY FURNISHED TO BDC



MAY 15 1979 9:36

TRANSFORM

| | 1 | 2 | 3 | 4 | 5 | 6 | 7 | 8 | 9 | 10 | 11 | 12 | 13 | 14 | 15 | 16 |
|----|---|----|----|----|----|---|----|----|---|----|----|----|----|----|----|----|
| 1 | 9 | -9 | -8 | 8 | -9 | 9 | 8 | -8 | 3 | -3 | -2 | 2 | -3 | 3 | 2 | -2 |
| 2 | 0 | 0 | 0 | 0 | 0 | 0 | 0 | 0 | 1 | -1 | 0 | 0 | -1 | 1 | 0 | 0 |
| 3 | 0 | 0 | 1 | -1 | 0 | 0 | -1 | 1 | 0 | 0 | 0 | 0 | 0 | 0 | 0 | 0 |
| 4 | 0 | 0 | 0 | 0 | 0 | 0 | 0 | 0 | 1 | -1 | 0 | 0 | -1 | 1 | 0 | 0 |
| 5 | 0 | 0 | 0 | 0 | 0 | 0 | 0 | 0 | 0 | 0 | 0 | 0 | 0 | 0 | 0 | 0 |
| 6 | 0 | 0 | 0 | 0 | 0 | 0 | 0 | 0 | 0 | 0 | 0 | 0 | 0 | 0 | 0 | 0 |
| 7 | 0 | 0 | 0 | 0 | 0 | 0 | 0 | 0 | 0 | 0 | 0 | 0 | 0 | 0 | 0 | 0 |
| 8 | 0 | 0 | 0 | 0 | 0 | 0 | 0 | 0 | 0 | 0 | 0 | 0 | 0 | 0 | 0 | 0 |
| 9 | 0 | 0 | 0 | 0 | 0 | 0 | 0 | 0 | 0 | 0 | 0 | 0 | 0 | 0 | 0 | 0 |
| 10 | 0 | 0 | 0 | 0 | 0 | 0 | 0 | 0 | 0 | 0 | 0 | 0 | 0 | 0 | 0 | 0 |
| 11 | 0 | 0 | 0 | 0 | 0 | 0 | 0 | 0 | 0 | 0 | 0 | 0 | 0 | 0 | 0 | 0 |
| 12 | 0 | 0 | 0 | 0 | 0 | 0 | 0 | 0 | 0 | 0 | 0 | 0 | 0 | 0 | 0 | 0 |
| 13 | 0 | 0 | 0 | 0 | 0 | 0 | 0 | 0 | 0 | 0 | 0 | 0 | 0 | 0 | 0 | 0 |
| 14 | 0 | 0 | 0 | 0 | 0 | 0 | 0 | 0 | 0 | 0 | 0 | 0 | 0 | 0 | 0 | 0 |
| 15 | 0 | 0 | 0 | 0 | 0 | 0 | 0 | 0 | 0 | 0 | 0 | 0 | 0 | 0 | 0 | 0 |
| 16 | 0 | 0 | 0 | 0 | 0 | 0 | 0 | 0 | 0 | 0 | 0 | 0 | 0 | 0 | 0 | 0 |

VERTICAL LINE ROAD

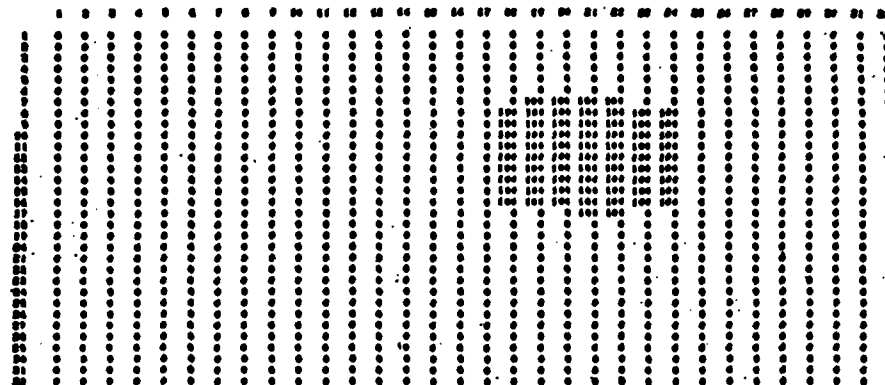
Figure 5. Spatial Signal Signature, Walsh Transform, and Classification Result for Vertical Line Road.

*CHEN and SEEMULLER

THIS PAGE IS BEST QUALITY PRACTICABLE
FROM COPY FURNISHED TO BDC

001 00 0000 001 4

00001



MAY 15 1979 10: 4

TRANSFORM

| | 1 | 2 | 3 | 4 | 5 | 6 | 7 | 8 | 9 | 10 | 11 | 12 | 13 | 14 | 15 | 16 |
|----|----|----|----|----|----|---|---|----|----|----|----|----|----|----|----|----|
| 1 | 6 | -6 | -6 | 6 | -1 | 1 | 1 | -1 | -1 | 1 | 1 | -1 | 0 | 0 | 0 | 0 |
| 2 | 6 | -6 | -6 | 6 | 0 | 0 | 0 | 0 | -1 | 1 | 1 | -1 | -1 | 1 | 1 | -1 |
| 3 | -4 | 4 | 4 | -4 | 0 | 0 | 0 | 0 | 0 | 0 | 0 | 0 | 0 | 0 | 0 | 0 |
| 4 | -4 | 4 | 4 | -4 | 0 | 0 | 0 | 0 | 0 | 0 | 0 | 0 | 0 | 0 | 0 | 0 |
| 5 | 0 | 0 | 0 | 0 | 0 | 0 | 0 | 0 | 0 | 0 | 0 | 0 | 0 | 0 | 0 | 0 |
| 6 | -1 | 1 | 1 | -1 | 0 | 0 | 0 | 0 | 0 | 0 | 0 | 0 | 0 | 0 | 0 | 0 |
| 7 | -1 | 1 | 1 | -1 | 0 | 0 | 0 | 0 | 0 | 0 | 0 | 0 | 0 | 0 | 0 | 0 |
| 8 | 0 | 0 | 0 | 0 | 0 | 0 | 0 | 0 | 0 | 0 | 0 | 0 | 0 | 0 | 0 | 0 |
| 9 | 1 | -1 | -1 | 1 | 0 | 0 | 0 | 0 | 0 | 0 | 0 | 0 | 0 | 0 | 0 | 0 |
| 10 | 0 | 0 | 0 | 0 | 0 | 0 | 0 | 0 | 0 | 0 | 0 | 0 | 0 | 0 | 0 | 0 |
| 11 | 0 | 0 | 0 | 0 | 0 | 0 | 0 | 0 | 0 | 0 | 0 | 0 | 0 | 0 | 0 | 0 |
| 12 | 1 | -1 | -1 | 1 | 0 | 0 | 0 | 0 | 0 | 0 | 0 | 0 | 0 | 0 | 0 | 0 |
| 13 | 0 | 0 | 0 | 0 | 0 | 0 | 0 | 0 | 0 | 0 | 0 | 0 | 0 | 0 | 0 | 0 |
| 14 | -1 | 1 | 1 | -1 | 0 | 0 | 0 | 0 | 0 | 0 | 0 | 0 | 0 | 0 | 0 | 0 |
| 15 | -1 | 1 | 1 | -1 | 0 | 0 | 0 | 0 | 0 | 0 | 0 | 0 | 0 | 0 | 0 | 0 |
| 16 | 0 | 0 | 0 | 0 | 0 | 0 | 0 | 0 | 0 | 0 | 0 | 0 | 0 | 0 | 0 | 0 |

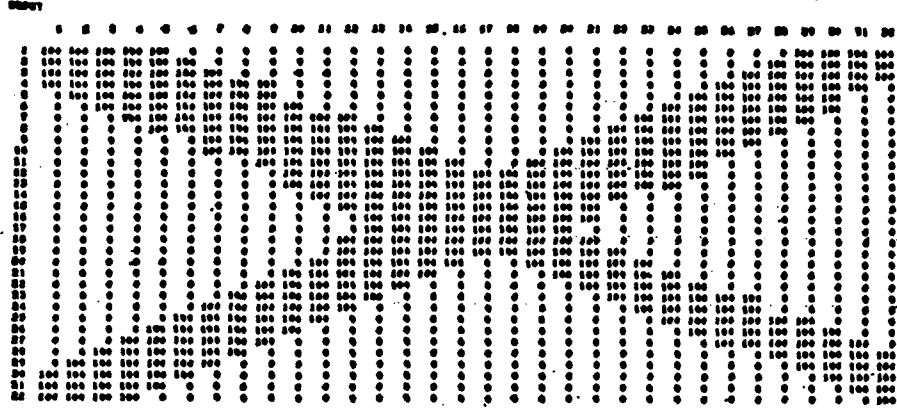
RECTANGULAR OBJECT

Figure 6. Spatial Signal Signature, Walsh Transform, and Classification Result for Rectangular Object.

*CHEN and SEEMULLER

THIS PAGE IS BEST QUALITY PRACTICAL
FROM COPY FURNISHED TO EDC

MAY 15 1979 00:11



MAY 15 1979 10:31

TRANSFORM

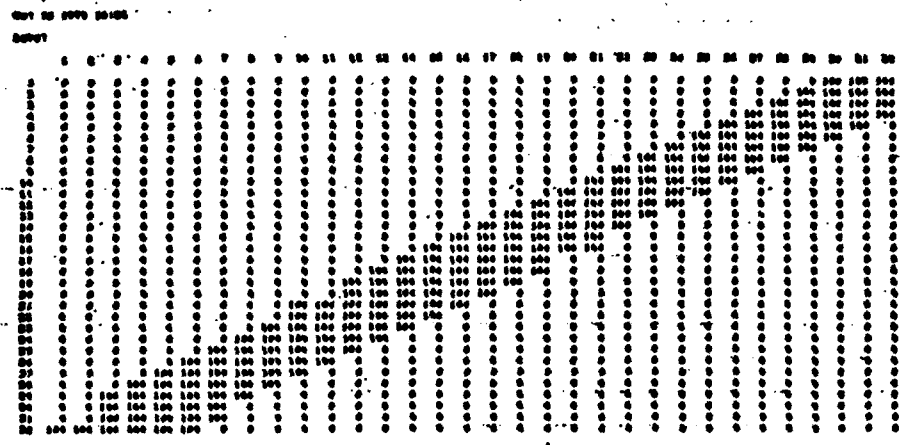
| | 1 | 2 | 3 | 4 | 5 | 6 | 7 | 8 | 9 | 10 | 11 | 12 | 13 | 14 | 15 | 16 |
|----|----|----|----|----|----|----|----|----|----|----|----|----|----|----|----|----|
| 1 | 37 | 2 | -1 | -1 | -3 | 0 | 0 | -1 | -2 | 0 | 0 | 0 | -2 | 0 | 0 | 0 |
| 2 | 5 | 0 | -1 | 0 | -1 | 0 | 0 | 0 | 0 | 0 | 0 | 0 | 0 | 0 | 0 | 0 |
| 3 | 0 | 2 | 27 | 1 | 0 | -4 | 4 | 0 | 0 | 0 | -8 | 0 | 0 | 0 | 2 | 0 |
| 4 | 0 | 0 | 2 | 0 | -2 | 0 | 0 | 1 | 0 | 0 | -1 | 1 | 0 | 0 | 0 | 0 |
| 5 | -4 | 0 | 0 | 4 | 17 | 0 | 0 | 0 | -2 | 0 | 0 | -2 | 0 | 0 | 0 | 0 |
| 6 | 0 | -1 | 3 | -1 | 0 | -1 | 0 | 0 | 0 | 1 | -1 | 1 | 0 | 0 | 0 | 0 |
| 7 | 0 | 1 | 3 | 0 | 0 | 2 | 9 | 0 | 1 | -2 | 2 | 0 | 0 | 0 | 2 | 0 |
| 8 | 1 | 0 | 1 | 0 | 2 | 0 | -1 | -1 | 0 | 2 | 0 | 0 | 0 | 0 | 0 | 0 |
| 9 | -2 | 0 | 0 | -1 | -2 | 0 | -1 | 2 | 3 | 0 | 0 | 1 | -1 | 0 | 0 | 0 |
| 10 | 0 | 0 | 0 | 0 | 0 | 0 | 1 | -3 | -1 | -1 | 1 | 0 | 0 | 0 | 0 | 0 |
| 11 | 0 | 0 | -7 | 0 | 0 | 1 | 2 | 0 | 0 | 0 | 1 | 0 | 1 | 1 | 0 | 0 |
| 12 | 0 | 0 | 0 | 0 | 1 | -2 | 0 | 0 | 0 | -2 | 0 | 0 | 1 | 1 | 0 | -1 |
| 13 | -3 | 0 | 0 | 1 | 0 | 0 | 0 | 0 | -1 | 0 | -1 | -1 | 1 | 0 | 0 | 0 |
| 14 | 0 | 0 | 1 | 0 | 1 | 0 | 0 | 0 | 0 | 0 | -1 | -1 | 0 | 1 | 0 | 0 |
| 15 | 0 | 0 | 2 | 0 | 0 | 0 | 2 | 0 | 0 | 0 | 0 | 0 | 0 | 0 | -1 | 0 |
| 16 | 0 | 0 | 0 | 0 | 0 | 0 | 0 | 0 | 0 | 0 | 0 | 0 | -1 | 0 | 0 | 2 |

DIAGONALLY ORIENTED ROAD INTERSECTION

Figure 7. Spatial Signal Signature, Walsh Transform, and Classification Result for Diagonally Oriented Road Intersection.

*CHEN and SEEMULLER

THIS PAGE IS BEST QUALITY FROM COPY FURNISHED TO EDC



MAY 15 1979 10:56

TRANSFORM

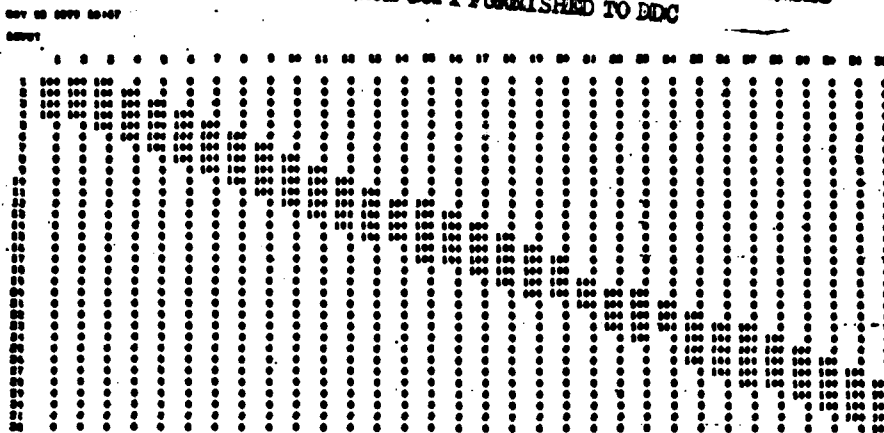
| | 1 | 2 | 3 | 4 | 5 | 6 | 7 | 8 | 9 | 10 | 11 | 12 | 13 | 14 | 15 | 16 |
|----|----|-----|----|-----|----|----|----|----|----|----|----|----|----|----|----|----|
| 1 | 18 | 0 | -2 | 0 | -1 | -1 | -2 | -1 | 0 | 0 | 0 | 0 | 0 | 0 | -1 | 0 |
| 2 | 0 | -16 | 2 | 0 | 0 | 3 | 2 | 0 | 0 | 2 | 0 | 0 | 0 | 2 | 0 | 0 |
| 3 | -1 | 1 | 14 | 0 | -3 | -3 | 2 | 0 | 0 | 0 | -3 | 0 | -1 | 0 | 1 | 0 |
| 4 | 0 | -1 | 0 | -12 | 4 | 0 | 0 | 0 | 0 | 0 | 0 | 0 | 4 | 0 | 0 | 0 |
| 5 | 0 | 0 | 0 | 3 | 9 | -1 | -2 | -1 | -1 | 0 | -1 | -1 | 4 | -1 | -1 | 0 |
| 6 | 0 | 2 | -2 | -2 | 0 | -7 | 2 | 0 | 0 | 2 | 2 | 0 | 0 | -2 | 0 | 0 |
| 7 | 0 | 1 | 3 | 0 | -1 | 0 | 5 | -2 | -1 | -2 | 1 | 0 | 0 | 0 | 1 | 0 |
| 8 | 0 | -1 | 0 | 0 | 0 | -1 | 0 | -3 | 2 | 0 | 0 | 0 | 0 | 0 | 0 | 0 |
| 9 | 0 | 0 | 0 | 0 | 0 | 0 | 0 | 1 | 2 | 0 | 0 | 0 | 0 | 0 | 0 | 0 |
| 10 | 0 | 1 | 0 | 0 | 0 | 1 | -1 | -1 | 1 | -2 | 0 | 0 | 0 | 0 | 0 | 0 |
| 11 | 0 | 0 | -2 | 0 | 0 | 1 | 1 | 0 | 0 | 0 | 0 | 1 | 0 | 0 | 0 | 0 |
| 12 | 0 | 0 | 0 | 3 | -1 | 0 | 0 | 0 | 0 | 0 | 0 | -1 | -1 | 0 | 1 | 0 |
| 13 | 0 | 0 | 0 | 1 | 3 | 0 | -1 | 0 | 0 | 0 | 0 | -1 | 0 | 1 | 0 | 0 |
| 14 | 0 | 1 | -1 | 0 | 0 | -2 | 0 | 0 | 0 | 0 | 0 | 0 | 0 | 0 | -1 | 0 |
| 15 | 0 | 0 | 2 | 0 | 0 | 0 | 1 | 0 | 0 | 0 | 0 | 0 | 0 | 0 | 0 | 2 |
| 16 | 0 | 0 | 0 | 0 | 0 | 0 | 0 | 0 | 0 | 0 | 0 | 0 | 0 | 0 | -1 | 0 |

DIAGONALLY ORIENTED LINE ROAD, 45 DEGREES

Figure 8. Spatial Signal Signature, Walsh Transform, and Classification Result for Diagonally Oriented Line Road (45 Degrees).

*CHEN and SEEMULLER

THIS PAGE IS BEST QUALITY PRACTICABLE
FROM COPY FURNISHED TO EDC



MAY 15 1979 10:47

TRANSFORM

| | 1 | 2 | 3 | 4 | 5 | 6 | 7 | 8 | 9 | 10 | 11 | 12 | 13 | 14 | 15 | 16 |
|----|----|----|----|----|----|----|----|----|----|----|----|----|----|----|----|----|
| 1 | 14 | 0 | 0 | 0 | 0 | 0 | 0 | 0 | 0 | 0 | 0 | 0 | 0 | 0 | 0 | 0 |
| 2 | 1 | 13 | -1 | 2 | 0 | -1 | 0 | 0 | 0 | -1 | 0 | 0 | 0 | -1 | 0 | 0 |
| 3 | -1 | 0 | 12 | 0 | 0 | -1 | 2 | 0 | -1 | 0 | -1 | 0 | 0 | 0 | 1 | 0 |
| 4 | 0 | 0 | 1 | 10 | -2 | 2 | 0 | 1 | 0 | 0 | 0 | -2 | -1 | 1 | 1 | 0 |
| 5 | -1 | 0 | -3 | 3 | 9 | 0 | 0 | 0 | 0 | 0 | 1 | -1 | 3 | 0 | 0 | 0 |
| 6 | 1 | -2 | 2 | -1 | 1 | 8 | 0 | 1 | 0 | 0 | -1 | 2 | 1 | 2 | 0 | 1 |
| 7 | -1 | 1 | 1 | 0 | -2 | 2 | 6 | 0 | 1 | -1 | 1 | 0 | 0 | 0 | 1 | 0 |
| 8 | 0 | 0 | 0 | 0 | 1 | 0 | 1 | 5 | -2 | 2 | 0 | 0 | 0 | 0 | 0 | 0 |
| 9 | 0 | 0 | 0 | 0 | -1 | 0 | -3 | 3 | 3 | 1 | 0 | 0 | 0 | 0 | 0 | 0 |
| 10 | 0 | -1 | 0 | 1 | 0 | -2 | 2 | -1 | 1 | 2 | 0 | 0 | 0 | -1 | 0 | 0 |
| 11 | -1 | 1 | -3 | 0 | -1 | 1 | 1 | 0 | 0 | 0 | 2 | 0 | 0 | 0 | 0 | 0 |
| 12 | 0 | 0 | 0 | -4 | 1 | 0 | 0 | 0 | 0 | 0 | 0 | 1 | 0 | 0 | 0 | 0 |
| 13 | 0 | 0 | -1 | 1 | 3 | 0 | 0 | 0 | 0 | -1 | 0 | 0 | 1 | 0 | 0 | 0 |
| 14 | 0 | -2 | 0 | 0 | 0 | 2 | 0 | 1 | -1 | 0 | 0 | 0 | 0 | 0 | 0 | 0 |
| 15 | 0 | 0 | 1 | 0 | -1 | 0 | 1 | 0 | 0 | 0 | 1 | 0 | 0 | 0 | 0 | -1 |
| 16 | 0 | 0 | 0 | 0 | 0 | 0 | 0 | 0 | 0 | 0 | 0 | 0 | 0 | 0 | -1 | 0 |

DIAGONALLY ORIENTED LINE ROAD, 135 DEGREES

Figure 9. Spatial Signal Signature, Walsh Transform, and Classification Result for Diagonally Oriented Line Road (135 Degrees).

*CHEN and SEEMULLER

to become a total automated feature extraction system.

AN ALTERNATE DETECTION SCHEME

In this section, an alternate scheme for detecting the decomposed spectral components (or Walsh transform coefficients) using analog processors is described. In the scheme, two cascaded, 32-stage programmable, binary-analog correlators [4] are used as shown in Figure 10. In the previous section it was shown that the significant spectral components in most cases appear in the first 8 by 8 lower order Walsh transform coefficients. Thus, two cascaded, 32-stage, binary-analog correlators should be sufficient to process the important coefficients to yield recognizable results. The Walsh transform coefficients are connected to the input of the analog delay line, and the binary patterns that represent reference signal signatures will be connected to the input of the static shift register. Each stage of the analog delay line has a pair of taps. These taps have switches in series with them that are controlled by the true and complement outputs of the static digital shift register. By loading a binary word to it, the static shift register will select the taps, which are connected to two output lines, thus proving the ability to do correlation. By sweeping the known binary words at a megahertz rate, the Walsh coefficients representing a particular type of feature will be quickly detected in the output of the operational amplifier.

The system described in the previous sections can be replaced by using this suggested scheme together with a solid state array, a hardware Walsh function generator, and some minor interface and display electronics. Although the analog method is relatively compact, it is much less flexible than the digital method described earlier.

CONCLUSIONS

1. The signal signature of the spectrally decomposed cartographic features is much simpler in distribution than the spatial signal signature of the same cartographic feature for all selected cases.
2. In most cases, the significant spectral components are distributed among few lower order Walsh transform coefficients. Further, each transform pattern is unique in itself, and it can be easily distinguished from the rest.
3. One or more reference signal signatures were required for each class of the selected set of cartographic features since they may

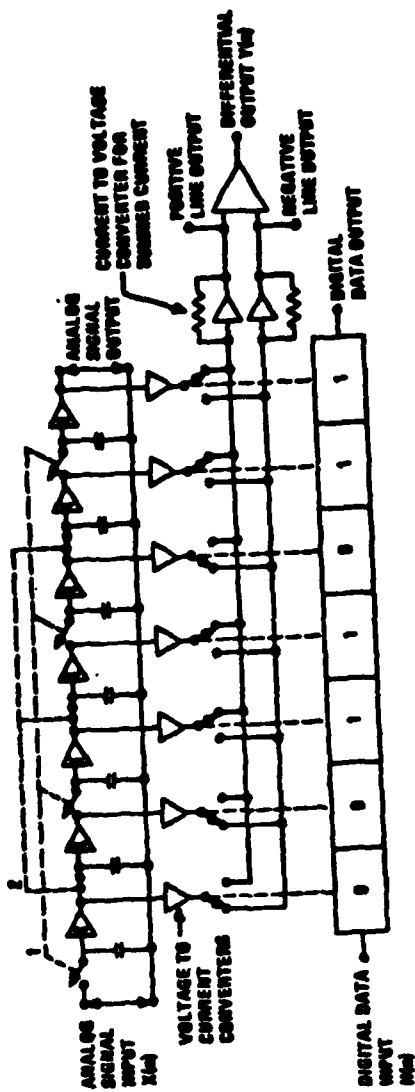


Figure 10. Alternate Detection Scheme.

*CHEN and SEEMULLER

appear in a variety of locations with respect to the window of inspection.

4. Four classes out of the entire seven cartographic feature classes selected were detected and recognized without error regardless of their locations with respect to the window. The rest of the feature classes were also classified correctly in a majority of locations. However, misclassifications occurred when these features were positioned very close to the corners of the window. Nearly 90 percent recognition accuracy was obtained for the selected set of the cartographic features.

5. The feature extraction scheme presented can also be implemented by using a group of analog signal processors together with the appropriate interfaces.

6. Image rotation may be incorporated in the future to refine the scheme for detecting these cartographic features at a variety of angles with respect to the axes of the window.

REFERENCES

- (1) P. F. Chen and W. W. Seemuller, "Signal Signatures of Topographic Features Using Analog Technology," USAETL Research Note No. ETL-0185, May 1979.
- (2) P. F. Chen, F. W. Rohde, and W. W. Seemuller, "Prototype Image Spectrum Analyzer (PISA) for Cartographic Feature Extraction," USAETL Research Note No. ETL-0204, Oct 1979.
- (3) H. F. Harmuth, "Sequency Theory, Foundation and Application," New York, Academic Press, Inc., 1977, pp 55-56.
- (4) V. Strasilla, "A Programmable Binary-Analog Correlator," Reticon Corporation, Sunnyvale, CA, Technical Note No. 106.